A small-angle X-ray scattering study of the annealing and gelatinization of starch*

R. E. Cameron† and A. M. Donald

Cavendish Laboratory, University of Cambridge, Madingley Road, Cambridge, CB3 0HE, UK

The structure of starch in its native state and during gelatinization was studied using small-angle X-ray scattering (SAXS). The scattering data were then modelled by considering the theoretical scattering from a finite number of infinite lamellar planes of crystalline and amorphous material, embedded in a medium of specified electron density. The changes in the SAXS pattern during gelatinization could be modelled simply by changing the relative electron densities of the system, thereby observing directly the absorption of water and the disruption of crystallinity. This rigorous analysis of the SAXS data from starch has provided new insights into the structure of native starch and the mechanisms of gelatinization.

(Keywords: lamellar structures; small-angle X-ray scattering; starch; gelatinization)

INTRODUCTION

Starch is composed of two polymers of glucose units: the highly branched amylopectin and its essentially linear counterpart, amylose. It is laid down in plants in the form of insoluble granules, those of wheat starch being of approximately 10 μm radius. The granules exhibit a birefringence, which reflects the intrinsic semicrystalline nature of starch in its native state. The crystallinity arises mainly from the branched amylopectin component[1,2], which is radially oriented in the granule. A variety of physical techniques have been employed by previous researchers to determine the structure. Enzymatic degradation studies on amylopectin suggest that it has a racemose structure, with heavily branched regions connecting with straight-chain, unbranched regions[3]. In the straight-chain regions, the chains form double helices with each other, which are about 60 Å in length. These double helices then pack together to form crystalline layers or lamellae. Wide-angle X-ray scattering (WAXS) has revealed the presence of three forms of packing of the helices, the so-called A, B and C forms[4–7]. In wheat starch, the crystallinity is of the A form. In between these crystalline layers, the branched material forms amorphous lamellae. When hydrated starch is viewed with small-angle X-ray scattering (SAXS)[8–10], a peak is seen at a value of q of 0.063 Å^{-1}. This peak is thought to arise from the alternating crystalline and amorphous lamellae of amylopectin. It is not seen in dry starch, which implies that the electron density difference between amorphous and crystalline starch is insufficient to scatter X-rays. In hydrated starch, the necessary electron density difference is due to preferential absorption of water into the amorphous regions within the structure, thereby lowering their electron density. The peak at 0.063 Å^{-1} can also be seen using small-angle neutron scattering[11] and by diffraction from electron micrographs[10].

In the plant, the growth of these lamellae forms a daily cycle. This results in the presence of 'growth rings', which can be observed by optical and electron microscopy. They consist of alternating concentric shells of semicrystalline material and largely amorphous material, and are due to the daily fluctuations in the amount of carbohydrate available as the starch granule grows in the plant. The relatively dense semicrystalline material consists of the amorphous and crystalline repeats of amylopectin. A single shell of this dense material has a thickness between about 1200 and 4000 Å (ref. 12). The largely amorphous shells are formed when there is less carbohydrate available, and contain more water and less starch than the dense layers. The thicknesses of these relatively amorphous shells are not reported, but electron micrographs seem to indicate that they are of comparable size to the dense regions. *Figure 1* shows a schematic representation of the amylopectin within a growth ring. The dimensions marked on this diagram are those arising from the research in this paper.

When heated to 50–60°C in excess water, starch undergoes a process known as gelatinization. Water is increasingly absorbed into the granule, which swells. The structure is disrupted and amylose leached out of the granule. The birefringence is lost and the WAXS diffraction pattern shows an amorphous profile. After complete gelatinization the peak in the SAXS intensity profile is no longer present[13]. This is the familiar process of cooking starch, as seen for example in the thickening of a sauce. The process can be observed as an endotherm by differential scanning calorimetry (d.s.c.).

EXPERIMENTAL METHOD

Slurries of wheat starch and water were sealed between two mica sheets with a brass spacer of width 0.25 mm. The mica was held in place by 'Devcon 5 mins epoxy'. The concentration of the slurries was 45% starch by weight. At this concentration there was sufficient starch

Growth Ring

88.5Å

66.5Å

1400Å = 16 repeats

**Amorphous shell
of growth ring**
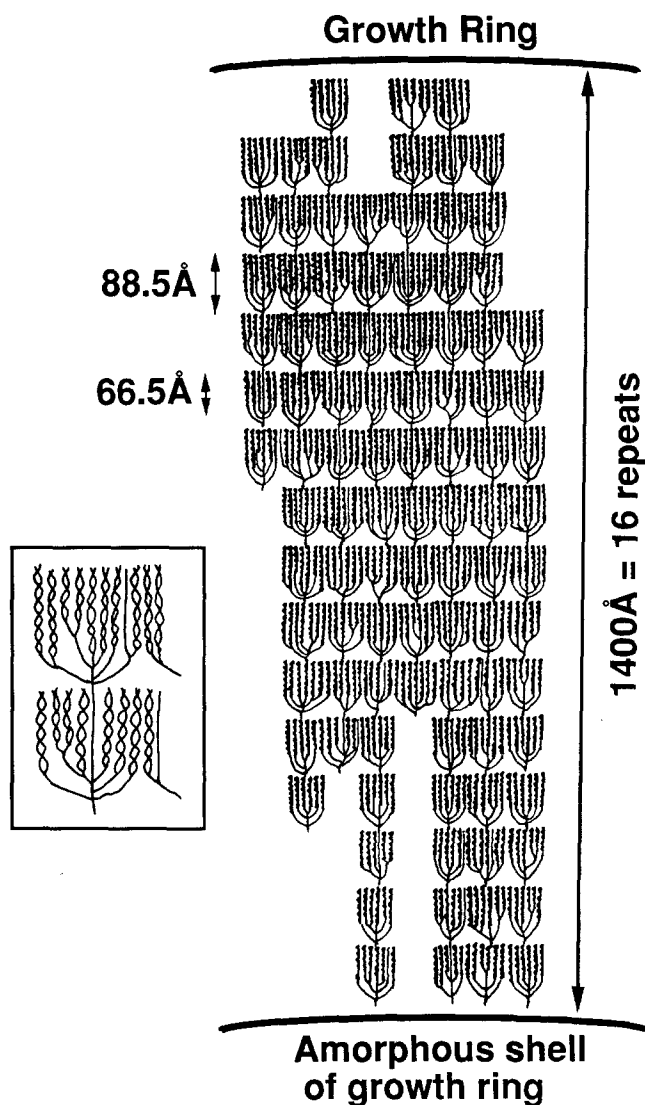
Figure 1 Schematic representation of the arrangement of amylopectin molecules within the dense shell of a growth ring. The inset shows individual clusters on a larger scale and illustrates the packing of the double helices. The dimensions shown are those obtained from the research presented here. (Adapted from ref. 12)

to prevent the suspension sinking within the cell. However, this concentration is sufficiently dilute to give excess water conditions for gelatinization[14].

The constant-temperature cell was constructed from brass. The temperature was controlled by pumping water from a water bath through the main body of the holder. A thermocouple inserted into the central brass section gave a readout of the temperature. Calibration experiments performed with a thermocouple sealed in water between mica sheets showed that the temperature at the centre of the sample cell reached the temperature of the central brass section about 2 min after insertion. Thereafter, the temperatures were the same.

The sample holder was allowed to equilibrate at the required temperature and the starch slurry sealed between mica discs was inserted. After 2 min equilibration time, data collection was started. Scattering experiments were performed on station 8.2 at the Synchrotron Radiatin Source at Daresbury. The high-intensity beam of Cu K_α radiation was collimated with slits and focused on a quadrant detector. The sample-to-detector distance was about 3 m. At this camera length, the vertical height

of the focused beam was 0.3 mm. The electronic pixel size of the detector, which determines vertical resolution, was 0.4–0.5 mm. The camera was therefore point collimated to within the resolution of the detector. Counts were recorded for 5 min into one file. After this 5 min the data were binned into a second file for 5 min and so on. A total of 12 files were recorded, thereby monitoring the intensity profile for 1 h. For some samples the beam was attenuated by placing a piece of photographic film in front of the detector. This prevented damage to the detector from high-intensity scattering.

The data were normalized, divided by the detector response, and the background scattering (as recorded by a blank sample cell) was subtracted. No desmearing is necessary because of the point collimation.

A 45% starch slurry held in the beam at room temperature for 1 h showed negligible change in comparison with the changes seen at elevated temperatures due to gelatinization. This implies that the changes in scattering due to beam damage of the sample were negligible on the scale of this experiment.

RESULTS AND DISCUSSION

Experimental results

Figures 2 and *3* show the intensity profiles of slurries of 45% starch at 51 and 61°C. Also plotted on these graphs is the profile of 45% starch at room temperature, the bottom curve on each graph. It will be seen that, at both temperatures, the definition of the peak is lowered
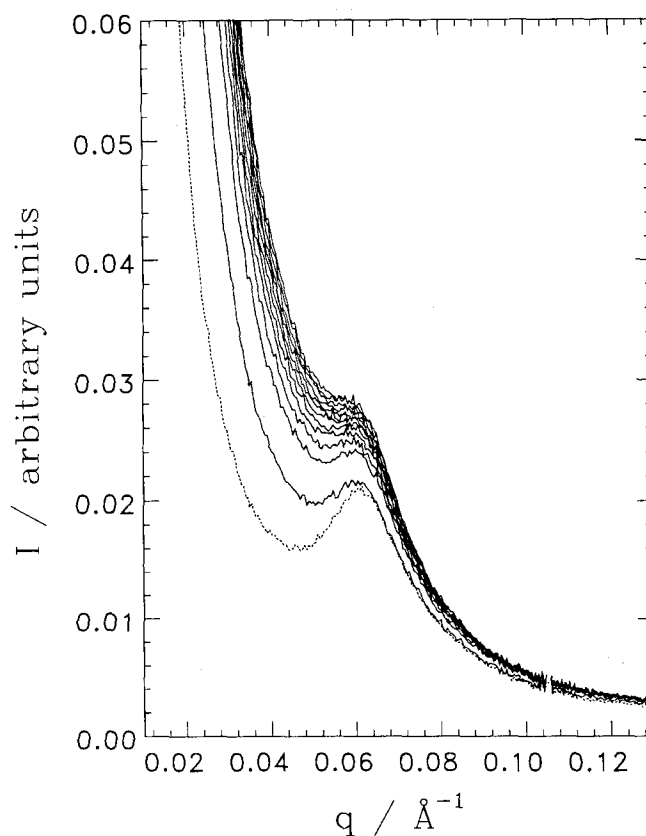
Figure 2 Changes in the SAXS intensity profile of a 45% starch slurry held at 51°C. The data are binned at 5 min intervals. Also shown is the profile of the sample at room temperature (dotted curve), which is the bottom curve on the plot. The low-angle intensity increases with time and the peak becomes progressively less well defined. All the curves at 51°C lie above that for native starch
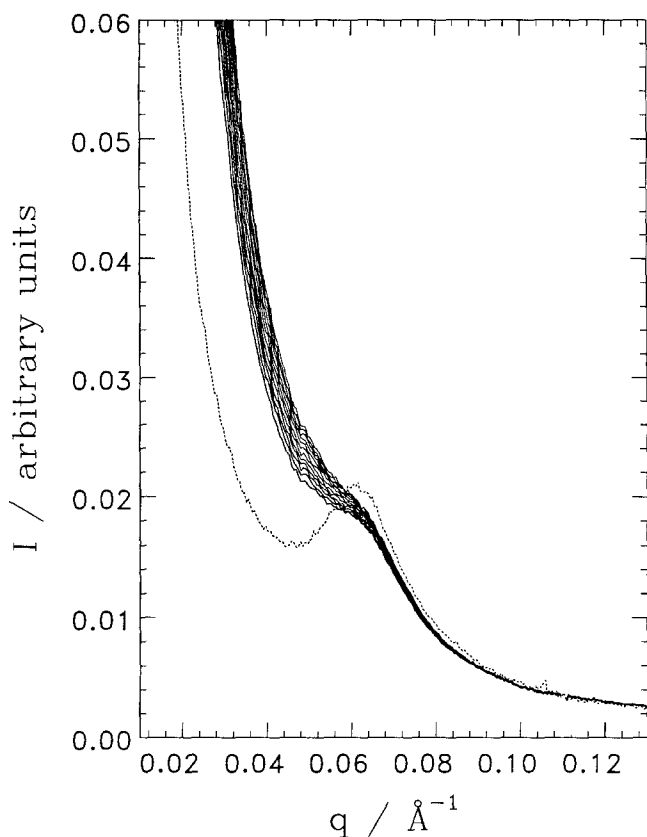
Figure 3 Changes in the SAXS intensity profile of a 45% starch slurry held at 61°C. The data are binned at 5 min intervals. Also shown is the profile of the sample at room temperature (dotted curve). The low-angle intensity increases with time and the peak becomes less well defined. Note that the curves fall below that for native starch

as time progresses, while the scattering at low angles increases. At 61°C the increase in scattering at low angles is less than that at 51°C, but the changes occur much more quickly. The peak at 61°C actually falls below the curve for room temperature. The peak is not completely removed at either temperature. Neither does it change position after any of the treatments, its q value remaining the same.

Theoretical analysis

A number of theoretical models for the structure of native starch were tried. Each used, as their basis, randomly oriented stacks of alternating layers of crystalline and amorphous material, each layer being of effectively infinite extent.

The first, and simplest, model was to take stacks of infinite extent, that is, each stack was an infinite number of alternating infinite planes of crystalline and amorphous material. This calculation requires five fitted parameters, four of which are varied: the average repeat distance, d; the crystallinity, ϕ; a factor related to the width of the distribution of lamellar thicknesses, β; and a y-axis fitting parameter. The final parameter, the electron density difference between the crystalline and amorphous material, $\Delta\rho$, is fixed at 1. However, it was not possible to obtain a satisfactory fit to the experimental data with this model.

Next, the number of repeats in a stack was limited to a finite number, N. This lamellar stack was assumed to be embedded in an infinite 'background' medium, with the same electron density as the amorphous material.

This model is known as the 'black–white' model[15], since, like the previous model, it contains two electron densities (black and white) and therefore only one electron density difference, $\Delta\rho$, taken to be 1. This model contains the additional parameter N, raising the number of variable parameters to five. Once again, however, it was not possible to obtain a reasonable fit to the experimental data.

The final, most complex, model attempted introduced one further parameter. This model is similar to the 'black–white' model of N repeats, but the background medium is no longer assumed to have the same electron density as the amorphous material. The electron density difference between the amorphous material and the background material, $\Delta\rho_u$, is the final fitting parameter. *Figures 4* and *5* show this schematically. Unlike the previous, simpler calculations, satisfactory fits were obtained using this six-parameter model. It thus seems that a minimum of three different electron densities are required to fit the experimental data. Despite the apparently large number of adjustable parameters employed, it is clear that fewer will not suffice. It is also important to note (as will be discussed more fully later) that to analyse the changes in signal during annealing and gelatinization only two of these parameters need to be varied, the other parameters remaining the same as for wheat starch at room temperature. The parameters of this model are now discussed in more detail.

The scattering from such a structure is given by the Fourier transform of the autocorrelation function of the
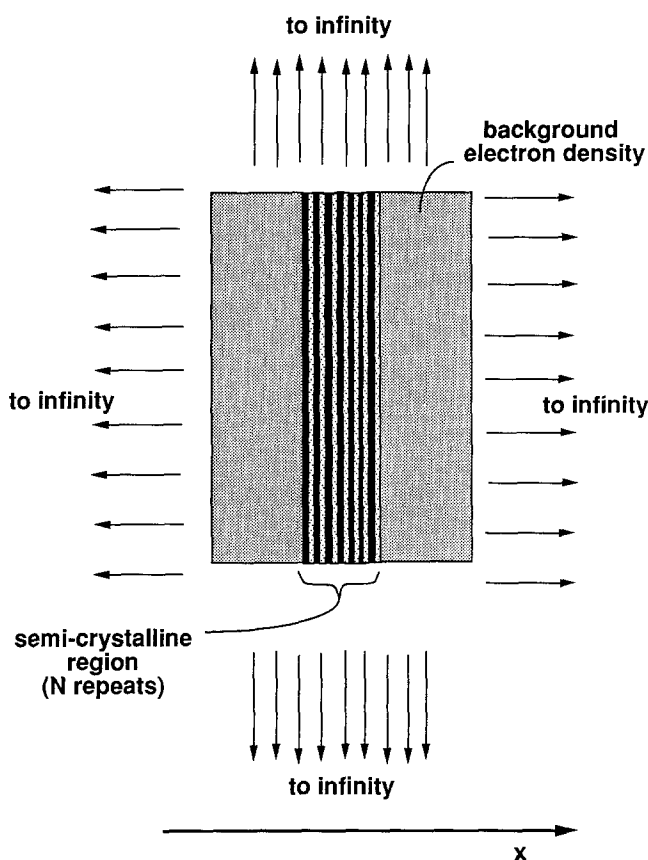
Figure 4 Schematic representation of the lamellar model used. The electron densities of the various regions are represented by the depth of shading. A finite number of infinite crystalline and amorphous lamellae are shown in the centre, surrounded by an infinite extent of background material
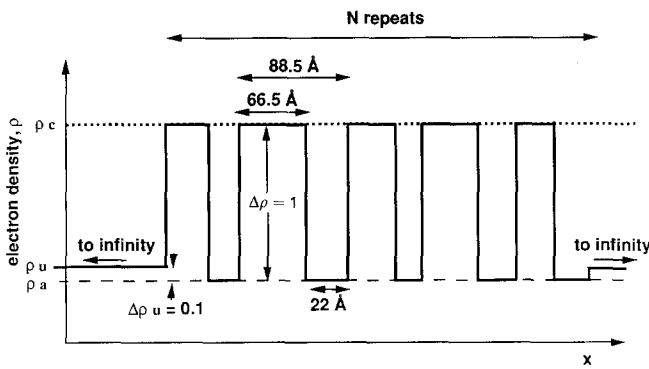
Figure 5 The electron density distribution of a finite lamellar stack embedded in a medium of electron density $\Delta\rho_u$. The electron density difference between the crystalline and amorphous lamellae is taken to be 1. The dimensions shown are those found from the fit to native starch. Only the electron density differences are found; the absolute values of ρ_c, ρ_a and ρ_u are not known

electron density distribution. Consider first the alternating layers of crystalline and amorphous material. The crystalline material has a higher electron density than the amorphous and this provides contrast for one component of the scattering for this model. This electron density difference:

$$\Delta\rho = \rho_c - \rho_a \qquad (1)$$

(where ρ_c and ρ_a are the electron densities of the crystalline and amorphous materials respectively) was arbitrarily taken to be 1 for native starch. The probability distribution functions of the crystalline and amorphous lamellar thicknesses $f_c(x)$ and $f_a(x)$ were assumed to be Gaussian[16], so for the crystalline regions:

$$f_c(x) = \left(\frac{1}{2\pi\Delta_c^2}\right)^{1/2} \exp\left(\frac{-(x - \langle x_c \rangle)^2}{2\Delta_c^2}\right) \qquad (2)$$

where Δ_c is the width of the distribution and $\langle x_c \rangle$ is the average thickness of the crystalline layers. The amorphous regions can be described similarly. If the crystallinity of the lamellar stack, ϕ, is defined as the proportion of material that is crystalline, and d is the average length of the overall repeat in the stack, then the average sizes of the lamellae can be written:

$$\langle x_c \rangle = \phi d \qquad \text{and} \qquad \langle x_a \rangle = (1 - \phi)d \qquad (3)$$

For simplicity in the calculation, the distribution thicknesses were assumed to be related to the average lamellar size[16]:

$$\Delta_c = \phi\beta d \qquad \text{and} \qquad \Delta_a = (1 - \phi)\beta d \qquad (4)$$

where β is a constant. Thus the width of the Gaussian describing the distribution of lamellar thicknesses is taken to be proportional to its midpoint. The larger the average size of the lamellae, the wider the distribution of sizes. (*Figure 6* shows the Gaussian distribution functions arising from the parameters determined for native starch at room temperature.)

Therefore, to describe the structure of the alternating layers of crystalline and amorphous material we have introduced three parameters: the average overall repeat distance, d; the crystallinity, ϕ; and a factor related to the widths of the distribution of the lamellar thicknesses, β. The electron density difference between the crystalline and amorphous phases, $\Delta\rho$, was taken to be 1 for native

starch. Two other parameters relating to the structure are considered. The number of pairs of crystalline and amorphous lamellae in the lamellar stack is taken to be a finite number, N. These N repeats are then embedded in an infinite 'background' medium of a specified electron density. The electron density difference between the amorphous material and the background material is another parameter:

$$\Delta\rho_u = \rho_u - \rho_a \qquad (5)$$

where ρ_u is the electron density of the background material. The finite extent of the lamellar region and the electron density of the background material provide a further source of scattering contrast. A final parameter is required in the fitting to map the y axis of the theoretical intensity onto the data. This parameter does not provide any useful information as the data intensities are recorded in arbitrary units.

The final equation that describes the scattering from a single stack of a finite number of infinite lamellae embedded in a medium of a specified electron density is then[15]:

$$
\begin{aligned}
I_1(q) = {} & \frac{2(\Delta\rho)^2}{q^2} \mathrm{Re}\left(\frac{(1 - F_c)(1 - F_a)}{(1 - F_cF_a)}\right. \\
& + \frac{1}{N}F_a\frac{(1 - F_c)^2}{(1 - F_cF_a)^2}\left[1 - (F_cF_a)^N\right] \Bigg) \\
& + \frac{2(\Delta\rho)^2}{q^2N}Re\left[\frac{(\Delta\rho_u)^2}{(\Delta\rho)^2}\left[1 - (F_cF_a)^N\right]\right. \\
& \left.- \frac{\Delta\rho_u}{\Delta\rho}\left((1 + F_a)\frac{(1 - F_c)}{(1 - F_cF_a)}\left[1 - (F_cF_a)^N\right]\right)\right]
\end{aligned}
$$
$$(6)$$

where $\Delta\rho$, $\Delta\rho_u$ and N are defined as above and $F_c(q)$ and $F_a(q)$ are the Fourier transforms of the thickness distribution functions $f_c(x)$ and $f_a(x)$. As Fourier transforms of Gaussians, $F_c(q)$ and $F_a(q)$ can be written in the form $A\,e^{i\theta}$. Therefore, with a considerable amount of algebraic manipulation, an analytic form of the above equation can be obtained, in terms of β, d, ϕ, N, $\Delta\rho$ and $\Delta\rho_u$.

This is the scattering from a single stack of lamellae. In practice, a sample will contain many such stacks,
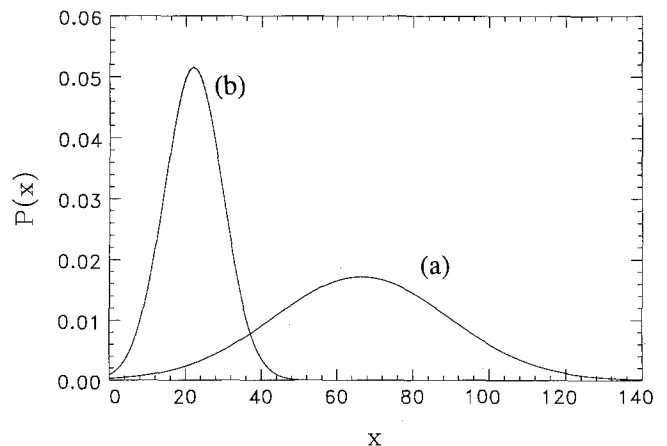
Figure 6 The probability distributions of the lengths of the (a) crystalline and (b) amorphous lamellae, corresponding to a value of β of 0.35, an overall repeat of 88.5 Å and a crystallinity of 0.75
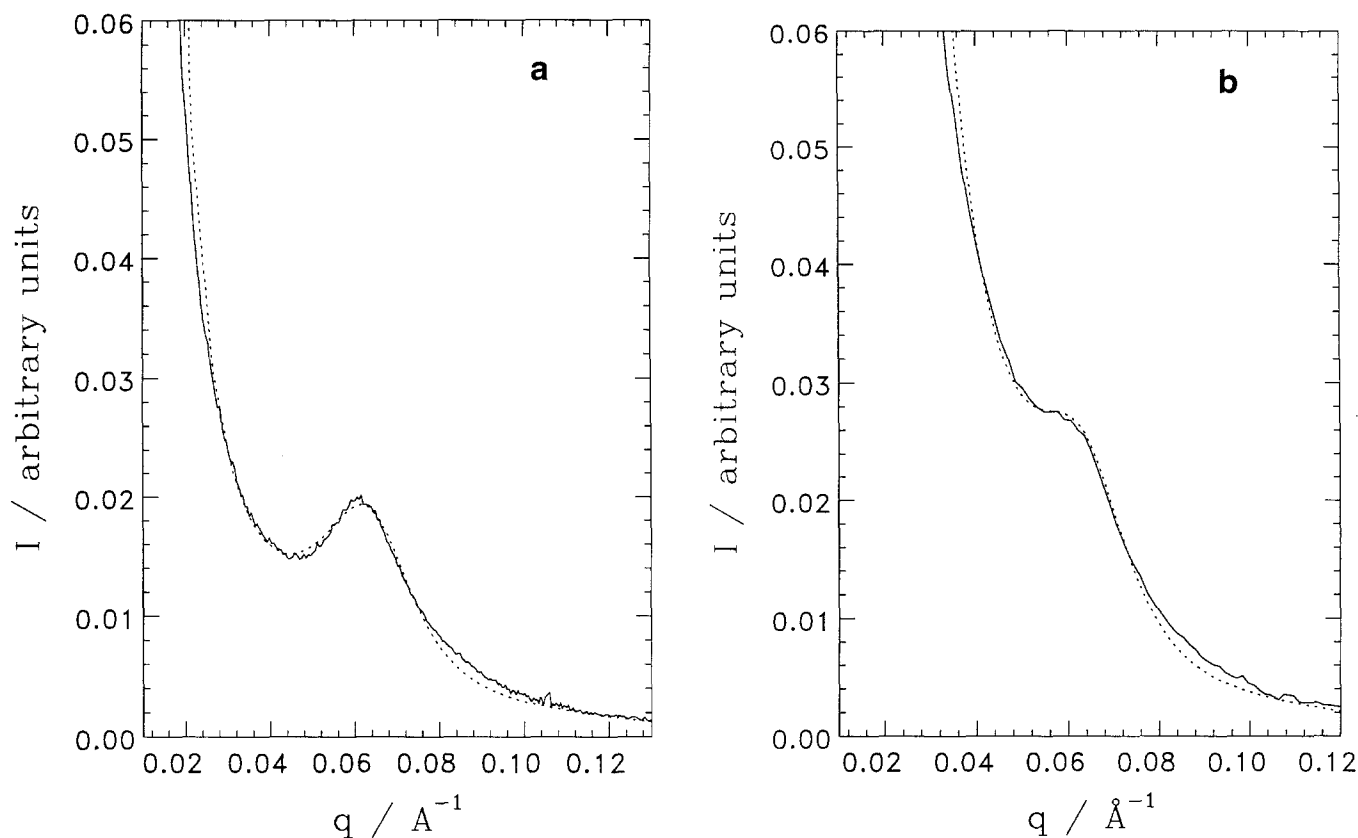
Figure 7 (a) The experimental data (full curve) and the theoretical fit (dotted curve) for 45% starch in water at room temperature. The parameters used are given in *Table 1*. (b) The experimental data (full curve) and the theoretical fit (dotted curve) for 45% starch in water after 55–60 min at 51°C

which will be oriented over all directions. The intensities of the stacks at a certain q value will be distributed in reciprocal space over the surface of a sphere of radius q. This means that the inteisity from the sample of non-oriented stacks will be given by:

$$I(q) = \frac{I_1(q)}{4\pi q^2} \qquad (7)$$

This is known as the Lorentz correction.

Fitting to the data

A least-squares fit was performed on the data using equation (6) with the Lorentz correction shown in equation (7). The experimental data fall to an approximately constant value at very high q values (around $0.2\,\text{Å}^{-1}$). This constant component of the scattering is due to 'liquid scattering' and should be subtracted from the curves before the fitting is attempted[17]. This constant value was subtracted from all curves prior to fitting.

For the fit to native starch at room temperature, the parameters β, d, ϕ, N and $\Delta\rho_u$ were varied in addition to the uninteresting y-axis fitting parameter. Only the data that lay around the peak (between about $q = 0.025$ and $q = 0.08\,\text{Å}^{-1}$) were used for the fit. The fit is shown in *Figure 7a* and the values determined are given in *Table 1*.

The parameters were then varied to model the changes that occur at elevated temperatures. Since all the data were normalized, the y-axis fitting parameter was held constant. The q value at which the peak occurred remained unchanged throughout temperature treatment,

Table 1

	β	d (A)	ϕ	N	$\Delta\rho$	$\Delta\rho_u$
Value	0.35	88.5	0.75	16	1	0.097

so parameters that move the peak position were held constant. This meant that the overall periodicity, d, the width of the distribution of lamellar thicknesses, β, and the number of repeats per stack, N, were not changed. The value of the crystallinity, ϕ, was also held constant. Changing this parameter has a strong effect on the high-angle regions of the curve, which remain essentially unchanged by the treatments. The remaining parameters were the two electron density differences $\Delta\rho$ and $\Delta\rho_u$. These two parameters were varied to fit the data obtained at elevated temperatures. Only the points around the peak were used, as for the data from native starch at room temperature. *Figure 7b* shows the fit to starch held at 51°C for 55–60 min. The major effect of increasing $\Delta\rho$, the electron density difference between the lamellar layers, is to increase the overall intensity. Increasing $\Delta\rho_u$, the electron density difference between the background and amorphous material, has the simultaneous effects of raising the low-angle intensity and lowering the definition of the peak without changing its position in q.

Interpretation of the parameters determined for wheat starch at room temperature

The value of the overall periodicity is calculated as 88.5 Å, a value different from the normally quoted value[8–11] of 100 Å. However, this discrepancy is a result

of the calculation method used by previous researchers, who have used the Bragg formula to obtain the figure of 100 Å. For lamellar systems, the q value at the peak maximum cannot be converted directly into a repeat distance via the Bragg formula unless the distribution of lamellar thicknesses is very narrow (implying a very small β). However, if a small value of β is used, then the shape of the peak is entirely different from that observed for starch. The form of the distribution required to fit the data is shown in *Figure 6* and is, in fact, rather broad. Therefore, since a distribution of thicknesses is present, the simple use of the Bragg formula must overestimate the overall repeat distance. (The value of 100 Å corresponds to a q value of 0.063 Å^{-1}, which is the position of the peak in *Figures 2* and *3*, so the experimental data are in agreement with earlier work.) The value of 100 Å *must* be too high since the shape of the experimental scattering curve is not consistent with a low β. Fitting using the lamellar model reported here shows that the true value is closer to 90 Å.

The relative lengths of the crystalline and amorphous layers are given by the crystallinity, $\phi = 0.75$. This implies that the ratio of thicknesses of crystalline and amorphous layers is 0.75:0.25. This corresponds to lengths of 66.4 and 22.1 Å. Published research[3], describing enzymatic degradation studies of amylopectin, gives an estimate for the lengths of the straight-chain portions of the amylopectin molecule. These studies have shown that the lengths of the double helices, which comprise the crystalline layers, lie in a broad distribution centred at around 60 Å.

The value of β of 0.35 describes the widths of the Gaussian distribution functions of crystalline and amorphous layer thicknesses. *Figure 6* shows these functions. It will be seen that the probability distribution function for the length of the crystalline phase is rather broad. So, although its peak position of 66 Å is rather higher than the figure of 60 Å suggested by enzymatic studies, the difference is relatively unimportant. Both the enzymatic studies and the X-ray results suggest a rather broad distribution of lengths, and the slightly differing peak positions of these distributions are probably not important.

The number of repeats per stack, N, was found to be 16 from this fit. The effect of changing this value by one or two repeats is small. Sixteen repeat units corresponds to a distance of about 1400 Å.

The value of $\Delta\rho$, the electron density difference between crystalline and amorphous regions, was taken to be 1. On the same scale, the value of $\Delta\rho_u$ was found to be 0.097. This implies that the electron density of the medium in which the lamellae are embedded is lower than the average electron density, yet higher than the value for amorphous material.

The model used implies the existence of three classes of material in the native starch. Simpler models that do not invoke this concept do not give satisfactory fits to the data. Crystalline and amorphous material is present in effectively infinite lamellae, which build up to regions about 16 repeats (or about 1400 Å) thick. The background material that surrounds these lamellar stacks is of an intermediate electron density, being higher than the amorphous material, but much lower than the crystalline.

As described earlier, the starch in a starch granule is laid down in concentric growth rings, which can be observed by optical and electron microscopy. These consist of alternating shells of semicrystalline material and largely amorphous material. It seems reasonable to identify the background material in the fitting model with the largely amorphous shells of the growth rings. In the model, the background material surrounds the stacks of crystalline and amorphous lamellae. These can be identified with the dense shells of the growth rings. The size of the lamellar stack confirms this interpretation of the model. According to the fit, the number of repeats in each stack was 16, corresponding to a distance of 1400 Å. This is comparable with the magnitude of the thickness of a dense shell of a growth ring reported in the published literature[12]. Because the amorphous shells form what is described by the fitting model as an infinite background material, the thicknesses of these shells must be at least as large as those of the dense shells.

According to the fit, the electron density of the amorphous material is slightly lower than that of the background material. It is reasonable to expect this since the amorphous lamellae are likely to contain a higher proportion of branched, and therefore lower-density, material. For the amorphous lamellae, any straight-chained material tends to crystallize in the adjacent crystalline regions.

Models that are simpler than the one used do not give satisfactory fits. Even with this rather complicated model, the fit is not perfect. Other still more complicated (but probably more realistic) models could be envisaged, for instance making the change in electron density at the various interfaces less abrupt. However, since we are interested not just in the native granule, but in the *changes* in its structure during annealing and gelatinization, when it is clear that water is entering the various regions of the granule and changing the electron densities, we have chosen to work with the simplest model that gives a reasonable fit to the data for the native granule. A comparison of *Figures 7a* and *7b* shows that, although the discrepancy between theory and experiment just below the peak and at high q is carried over after annealing, the change in the shape of the peak itself is well modelled. This indicates that, although the model is not correct in all its details, it does model the essence of the changes that are occurring.

Interpretation of the effect of temperature and time

The changes in the scattering intensity profile (shown in *Figures 2* and *3*) as the starch is held at elevated temperatures was modelled by changing the parameters $\Delta\rho$ and $\Delta\rho_u$. Parameter $\Delta\rho$ is the electron density difference between the crystalline and the amorphous material, that is $(\rho_c - \rho_a)$, and $\Delta\rho_u$ is that between the background and the amorphous material, $(\rho_u - \rho_a)$. It should be noted that both density differences are referenced to the amorphous material in *the sample under observation*. The absolute value of this is unlikely to remain constant throughout the experiment. That is, the reference value, ρ_a, will be changing throughout the experiment and the values of $\Delta\rho$ and $\Delta\rho_u$ only give information about the values of the electron densities of the crystalline and background regions relative to this changing value.

The values of $\Delta\rho$ and $\Delta\rho_u$ for the 45% starch in water sample held at 51°C show systematic changes. The value of $\Delta\rho$ rises slightly while $\Delta\rho_u$ becomes increasingly

Figure 8 Possible electron distribution functions for the fits obtained for 45% starch held at 51°C. The dotted lines and broken lines represent the electron densities of the crystalline and amorphous materials in the native starch at room temperature, i.e. ρ_{c0} and ρ_{a0}, respectively. The diagrams represent (a) native starch at room temperature, (b) 5–10 min at 51°C, (c) 20–25 min at 51°C and (d) 55–60 min at 51°C. The numbers are the electron density differences between marked levels

increase contrast, since the dry starch does not scatter X-rays while hydrated starch does.) Relative to the lowered value of ρ_a, the value of the background electron density, ρ_u, is reduced still further. This increase in contrast is interpreted as being due to ingress of water into the largely amorphous growth rings. It is clear from the large negative values of $\Delta\rho_u$ that this background region absorbs water to a much greater degree than the amorphous lamellae in the semicrystalline bulk. The amorphous lamellae in the bulk largely consist of branched regions of amylopectin molecules. Their freedom to swell and absorb water is severely constrained by the crystalline layers attached to them. In the background region there is a low degree of order over much longer length scales. Thus, this material is less constrained and more able to absorb water. *Figure 8* shows these changes in electron density schematically.

At 61°C, the absolute intensity of the peak is lowered, and it falls below that of the native starch at room temperature. This is a result of the values of $\Delta\rho$ actually falling below the value for the native starch. The implication is that the crystalline lamellae have been extensively disrupted, lowering the contrast between them and the amorphous lamellae despite the absorption of water into the latter. The values of $\Delta\rho_u$ are more negative than those found at 51°C, indicating that relative to the lowered value of $\Delta\rho_a$ the electron density of the background material is lowered still further. *Figure 9* shows possible absolute values.

It must be stressed that no information is gained about absolute electron densities from this analysis. The values of $\Delta\rho$ and $\Delta\rho_u$ are known, but their relation to the initial absolute values in the native starch at room temperature are not. This means that in *Figures 8* and *9* the shapes of the electron density distributions are correct, but their positions relative to ρ_{c0} and ρ_{a0} are to some extent conjecture, based on the reasoning given above.

Samples observed at temperatures between 51 and 61°C show intermediate behaviour.

From these studies it can be seen that the disruption of the crystalline lamellae occurs strongly at 61°C. The onset of this process may well be related to other observed properties of the granule during gelatinization such as the birefringence end point. Further experiments are planned to study the birefringence and the swelling, d.s.c. and amylose leaching properties of samples subjected to the treatments observed. Some d.s.c. work has been performed on similar treatment of rice starch[18], where the treatment was shown to change the position and shape of the gelatinization endotherm. Performing similar experiments under the conditions used here would be informative.

negative with increasing time at 51°C. The rise in $\Delta\rho$ implies that the density difference between the crystalline and amorphous lamellae is rising with time. Since the crystalline regions are unlikely to become more dense during this treatment, it is assumed that no density is ever higher than ρ_{c0}, the electron density of the crystalline lamellae at room temperature. The increase in $\Delta\rho$ must therefore be due to a lowering of the electron density of the amorphous lamellae. This is interpreted as water being absorbed preferentially into the amorphous regions, lowering their electron density. (The preferential ingress of water into amorphous regions is known to

CONCLUSIONS

The structure of wheat starch at room temperature and during gelatinization has been studied through analysis of SAXS data. The structure was modelled as consisting of a random array of stacks of infinite lamellae embedded in a medium of specified electron density. The values of the parameters determining the character and dimensions of the model were found from theoretical fits to the data. The lamellar repeat distance was found to be 88.5 Å, rigorous analysis of the data showing that the normally quoted value of 100 Å, found from simple application of the Bragg equation, is an overestimate. The crystallinity

ρ c

Δρ = 1

ρ u 0.1

1

ρ a

(a)

ρ c

0.87

ρ a

1.15

ρ u

(b)

ρ c

0.87

ρ a

1.27

ρ u

(c)

ρ c

0.86

ρ a

1.53

ρ u

(d)
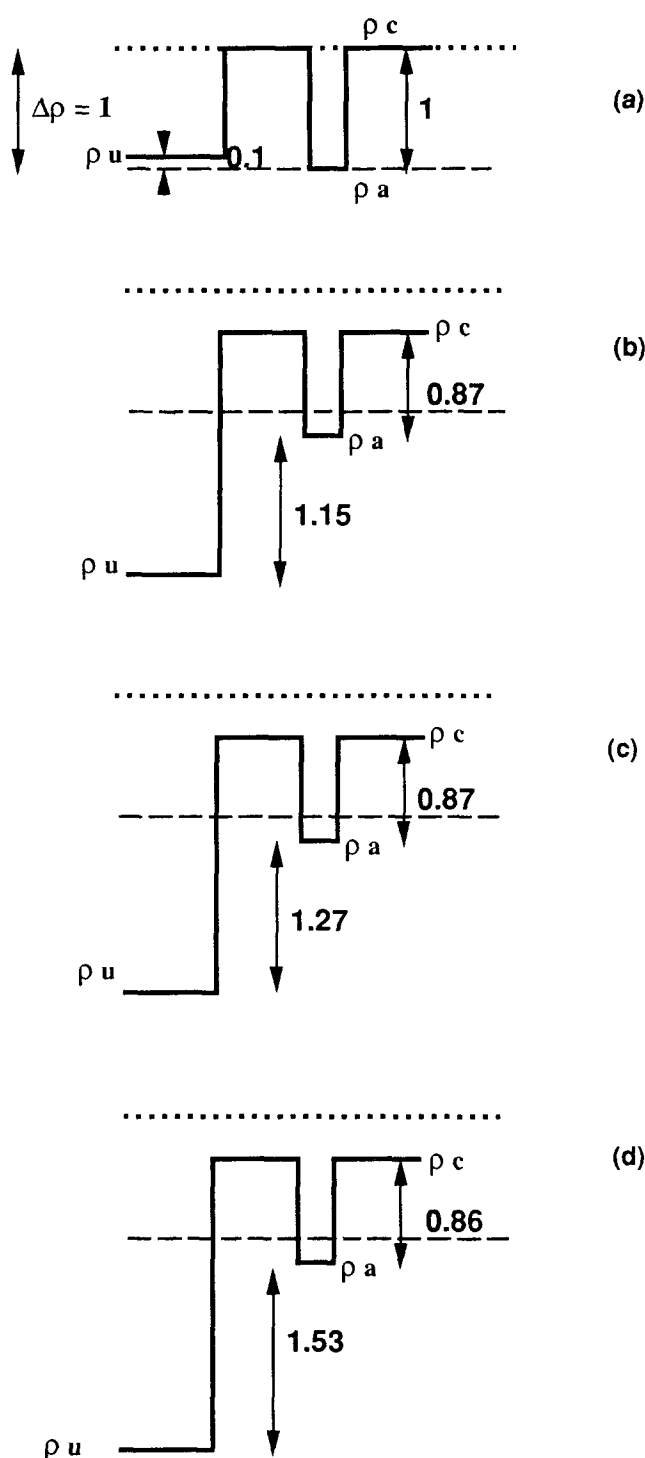
Figure 9 Possible electron distribution functions for the fits obtained for 45% starch held at 61°C. The dotted lines and broken lines represent the electron densities of the crystalline and amorphous materials in the native starch at room temperature, i.e. ρ_{c0} and ρ_{a0}, respectively. The diagrams represent (a) native starch at room temperature, (b) 5–10 min at 61°C, (c) 20–25 min at 61°C and (d) 55–60 min at 61°C. The numbers are the electron density differences between marked levels

of the lamellar stack was shown to be about 0.75, a value that leads to dimensions which agree with published data from enzymatic degradation. The number of repeats in each stack was found to be about 16, a figure that

corresponds to a distance of about 1400 Å corresponding to the size of the relatively dense material of a growth ring in starch. The embedding medium, interpreted as the amorphous material of a growth ring, has an electron density slightly higher than that of the amorphous lamellae, a fact attributed to the higher proportion of branched material in the latter.

Gelatinization was successfully modelled by varying the relative electron densities $\Delta\rho$ and $\Delta\rho_u$, the differences between the crystalline and the amorphous, and between the background and the amorphous electron densities respectively. At 51°C, the contrast between the crystalline and amorphous lamellae increased with time as water was absorbed into the amorphous lamellae. At 61°C, this contrast decreased, indicating that significant disruption of the crystalline material was taking place. At both temperatures, the large increase in $\Delta\rho_u$ showed that the background material absorbed water faster and to a greater extent than the amorphous lamellae, a fact attributed to the lower degree of physical constraint in this region.

REFERENCES

1 Meyer, K. H. *Adv. Colloid Sci.* 1942, **1**, 183
2 Montgomery, E. M. and Senti, F. R. *J. Polym. Sci.* 1958, **18**, 1
3 Robin, J. P., Mercier, C., Charbonniere, R. and Guilbot, A. *Cereal Chem.* 1974, **51**, 389
4 Katz, J. R. and Van Itallie, T. B. *Z. Phys. Chem. (A)* 1930, **150**, 90
5 Wu, H. C. and Sarko, A. *Carbohydr. Res.* 1978, **61**, 7
6 Wu, H. C. and Sarko, A. *Carbohydr. Res.* 1978, **61**, 27
7 Hizukiri, S. and Nikuni, Z. *Nature* 1957, **180**, 436
8 Stirling, C. *J. Polym. Sci.* 1962, **56**, S10
9 Muhr, A. H., Blanshard, J. M. V. and Bates, D. R. *Carbohydr. Polym.* 1984, **4**, 399
10 Oostergetel, G. T. and Van Bruggen, E. F. G. *Stärke* 1989, **41**, 331
11 Blanshard, J. M. V., Bates, D. R., Muhr, A. H., Worcester, D. L. and Higgins, J. S. *Carbohydr. Polym.* 1984, **4**, 427
12 French, D. 'Starch, Chemistry and Technology' (Eds. R. L. Whistler, J. N. BeMiller and E. F. Paschell), 2nd Edn, Academic Press, London, 1984, p. 208
13 Cameron, R. E. and Donald, A. M. 'Food Polymers, Gels and Colloids' (Ed. E. Dickinson), Royal Society of Chemistry, Cambridge, 1991, p. 301
14 Burt, D. J. and Russell, P. L. *Stärke* 1983, **35**, 354
15 Wenig, W. and Brämer, R. *Colloid Polym. Sci.* 1978, **256**, 125
16 Vonk, C. G. *J. Appl. Crystallogr.* 1978, **11**, 541
17 Vonk, C. G. personal communication, 1990
18 Nakazawa, F., Noguchi, S., Takahashi, J. and Takada, M. *Agric. Biol. Chem.* 1984, **48**(11), 2647